Journal of Hazardous Materials 429 (2022) 127746

Contents lists available at ScienceDirect

Journal of Hazardous Materials

journal homepage: www.elsevier.com/locate/jhazmat

Research Paper

Toxicity of 4-(methylnitrosamino)-1-(3-pyridyl)-1-butanone (NNK) in early development: A wide-scope metabolomics assay in zebrafish embryos

Carla Merino [a,b,c], Marta Casado [d], Benjamí Piña [d], Maria Vinaixa [a,b,c,*], Noelia Ramírez [a,b,c,**]

[a] Universitat Rovira i Virgili, Departament d'Enginyeria Electrònica, Elèctrica i Automàtica, Tarragona, Spain
[b] Institut d'Investigació Sanitària Pere Virgili, Tarragona, Spain
[c] CIBER de Diabetes y Enfermedades Metabólicas Asociadas (CIBERDEM), Instituto de Salud Carlos III, Madrid, Spain
[d] Department of Environmental Chemistry, Institute of Environmental Assessment and Water Research, Spanish Council for Scientific Research (IDAEA-CSIC), Barcelona, Spain

HIGHLIGHTS

- NNK, a ubiquitous tobacco specific toxicant, affects early development in zebrafish.
- NNK exposed zebrafish embryos activate detoxification and pro-carcinogenic pathways.
- NNK exposure enhances nucleotide biosynthesis and DNA base excision repair pathways.
- Zebrafish embryos are a suitable model to study NNK toxicity in early development.

GRAPHICAL ABSTRACT

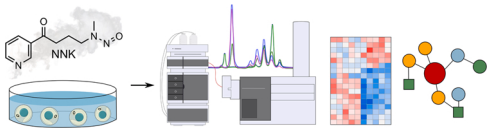

ARTICLE INFO

Editor: Dr. R Sara

Keywords:
4-(Methylnitrosamino)-1-(3-pyridyl)-1-butanone (NNK)
Danio rerio
Early development
Metabolomics
Nucleotide metabolism

ABSTRACT

The tobacco-specific nitrosamine 4-(Methylnitrosamino)-1-(3-pyridyl)-1-butanone (NNK) is a carcinogenic and ubiquitous environmental pollutant for which toxic activity has been thoroughly investigated in murine models and human tissues. However, its potential deleterious effects on vertebrate early development are yet poorly understood. In this work, we characterized the impact of NNK exposure during early developmental stages of zebrafish embryos, a known alternative model for mammalian toxicity studies. Embryos exposed to different NNK concentrations were monitored for lethality and for the appearance of malformations during the first five days after fertilization. LC-MS based untargeted metabolomics was subsequently performed for a wide-scope assay of NNK-related metabolic alterations. Our results revealed the presence of not only the parental compound, but also of two known NNK metabolites, 4-Hydroxy-4-(3-pyridyl)-butyric acid (HPBA) and 4-(Methylnitrosamino)-1-(3-pyridyl-N-oxide)-1-butanol (NNAL-*N*-oxide) in exposed embryos likely resulting from active CYP450-mediated α-hydroxylation and NNK detoxification pathways, respectively. This was paralleled by a disruption in purine and pyrimidine metabolisms and the activation of the base excision repair pathway. Our results confirm NNK as a harmful embryonic agent and demonstrate zebrafish embryos to be a suitable early development model to monitor NNK toxicity.

* Correspondence to: URV, Department of Electronic Engineering, Av. Països Catalans, 26, 43007 Tarragona, Spain.
** Correspondence to: IISPV-URV-CIBERDEM, Av. Països Catalans, 26, 43007 Tarragona, Spain.
E-mail addresses: maria.vinaixa@urv.cat (M. Vinaixa), noelia.ramirez@iispv.cat (N. Ramírez).

https://doi.org/10.1016/j.jhazmat.2021.127746
Received 8 June 2021; Received in revised form 29 October 2021; Accepted 8 November 2021
Available online 14 November 2021

1. Introduction

The World Health Organization (WHO) recognizes exposure to tobacco smoke toxicants as a major environmental health issue affecting both smokers and passive smokers such as young children (World Health Organization, 2017). Almost half of children regularly breathe air polluted with tobacco smoke in public places and 65,000 die each year from illnesses attributable to secondhand smoke (SHS), which has been related to pregnancy complications and low birth weight (World Health Organization, 2020), as well as, to respiratory diseases, neurodevelopmental alterations, and increased risk of sudden infant death syndrome (U.S. Department of Health and Human Services et al., 2014). Beyond SHS, the so-called thirdhand smoke (THS) is considered as another form of passive exposure to residues of tobacco smoke that deposits, ages, and remains in fabrics, surfaces, and settled dust particles long after smoking has ceased (Matt et al., 2011).

The tobacco specific nitrosamine 4-methylnitrosamino-1-(3-pyridyl)-1- butanone (NNK) is one of the most abundant and strongest carcinogens in SHS and THS (Hecht and Hoffmann, 1988; Jacob et al., 2017; Schick and Glantz, 2007), being classified as Group 1 carcinogenic in humans by the International Agency for Research on Cancer (IARC) (International Agency for Reasearch on Cancer, 2007). NNK is formed upon the oxidation of residual nicotine from tobacco smoke with nitrous acid, ozone, and other atmospheric oxidants (Sleiman et al., 2010). NNK has been ubiquitously detected in settled dust, even in some smoke-free homes (Ramírez et al., 2014), outdoor airborne particulate matter (Farren et al., 2015), waste waters (Lai et al., 2018) and river waters (Wu et al., 2012) expanding NNK exposure to non-smoking population such as children. Relevant NNK toxicity studies have traditionally focused on its associated carcinogenicity in adult animal models. Thus, NNK has been evaluated in vitro in cultured explants and epithelial cells of human buccal mucosa, and in vivo in murine models where it has been demonstrated to cause tumours in nasal cavities, trachea, lung, liver, stomach, and skin (Hecht, 1998). DNA adduct formation drives these malignant transformations, a process triggered by NNK metabolic activation occurring via P450-mediated carbonyl reduction, pyridine oxidation, α-hydroxylation of the carbons adjacent to the N-nitroso group, denitrosation, and ADP adduct formation (Balbo et al., 2014). However, NNK toxicity effects during early life remain less studied even though children are considered particularly vulnerable, and their exposure dose has been estimated higher than among adults (Wei et al., 2016). Some perinatal toxicity assays in murine models have demonstrated NNK to be a weak (transplacentally in mice) to moderate (neonatal mice and transplacentally in hamsters) perinatal carcinogen crossing the placental barrier and causing tumours in the offspring of exposed pregnant rodents (Anderson et al., 1991, 1989; Correa et al., 1990; Rossignol et al., 1989). NNK has also been shown to be a weak embryotoxic and teratogenic agent in mice models (Winn et al., 1998). However, mechanisms underlying such NNK toxic effects during early development remain yet to be fully elucidated.

In this context, the use of alternative animal models and the adoption of systems-wide approaches to assay toxicity has been put forward to meet the twenty-first century guidelines on toxicity testing (Hartung, 2009; National Research Council, 2007). Zebrafish (*Danio rerio*) have emerged as an excellent vertebrate alternative model granting low-cost and high-throughput toxicological assays during developmental biology and embryogenesis. The developing zebrafish embryo has been suggested as a relevant model to screen for potential teratogens due to genetic conservation with mammals, experimental advantages over higher vertebrates, and external development of transparent embryos, among others (Jarque et al., 2020; Lieschke and Currie, 2007; Sipes et al., 2011). Additionally, metabolomics, that is, the comprehensive measurement of metabolites in a biological specimen, can provide a direct and functional readout of an organism phenotype allowing a deeper understanding of the mode(s) and mechanism(s) of action of toxicity in human and environmental health (Ramirez et al., 2013). The goal of this exploratory study is twofold: to unveil the potential metabolic disruptions caused by NNK exposure at early developmental stages using a systemic toxicity assay based on a wide-scope metabolism interrogation through mass spectrometry-based untargeted metabolomics; and to assess whether zebrafish embryos can be used as an alternative model for NNK toxicity testing in early development.

2. Materials and methods

2.1. Chemicals and reagents

4-(Methylnitrosamino)-1-(3-pyridyl)-1-butanone (NNK) was obtained from LGC-Dr Ehrenstorfer (LGC Standards, Barcelona, Spain) and 4-Hydroxy-4-(3-pyridyl)-butyric acid (HPBA) was purchased from Toronto Research Chemicals (TRC, Ontario, Canada). The metabolites hypoxanthine, cytidine monophosphate (CMP), guanosine monophosphate (GMP), S-adenosylmethionine (SAM), and uridine monophosphate (UMP) were obtained from Sigma-Aldrich (Sigma-Aldrich, St. Louis, MO, USA). Internal standard (IS) solution was prepared with 1 mg mL^{-1} of succinic-d_4 acid and myristic-d_{27} acid in methanol also from Sigma-Aldrich. All solvents used in the preparation of solutions were LC-MS grade. Fish water was prepared with reverse-osmosis purified water containing 90 μg mL^{-1} of Instant Ocean®, 0.58 mM $CaSO_4{\cdot}2H_2O$ (Aquarium Systems, Sarrebourg, France).

2.2. Zebrafish maintenance and embryo collection

Wildtype zebrafish (*Danio rerio*) embryos were obtained by natural mating of 3 males and 5 females on 4 L mesh-bottom breeding tanks. At 2 h post-fertilization (hpf), viable fertilized eggs were collected, rinsed with fish water, and kept in clean fish water under standard conditions (28.5 °C and 12 h Light:12 h Dark photoperiod) until the day of exposure. Embryos were incubated under the same conditions during all the experiment. All procedures were conducted in accordance with the institutional guidelines under a license from the local government (DAMM 7669, 7964) and were approved by the Institutional Animal Care and Use Committees at the Research and Development Centre of the Spanish Research Council, CID-CSIC.

2.3. NNK exposure setup

At 48 hpf, zebrafish embryos were exposed in pools of 10 individuals to either fish water (control group) or to a gradient of NNK dilutions in fish water (50, 100, 150, and 200 μM) using a total of 500 embryos for the study. NNK exposure concentrations were based on those previously tested in vitro assays (Cheng et al., 2015; Hang et al., 2013; Weng et al., 2018; Winn et al., 1998) and those described for murine models exposed to TSNAs through drinking water (Balbo et al., 2014, 2013). Medium containing freshly prepared NNK solutions was renewed daily to ensure NNK continuous exposure. Anatomical development of embryos was followed daily under stereomicroscope Nikon SMZ1500 equipped with a Nikon digital Sight DS-Ri1 camera. Embryos were monitored and classified into three categories according to their phenotype: normal phenotype, severe phenotype (non-hatched embryos, oedema, and other morphological anomalies) and dead embryos at 72, 96 and 120 hpf. Developmental effects considered in the classification of embryo phenotypes are listed in Table S1 of the Supplementary information. At 120 hpf, larvae exposed to the same NNK concentrations were randomized and split into five biological replicates containing 17–20 larvae each. These were rinsed with egg water (60 μg mL^{-1} of Instant Ocean® sea salts in reverse-osmosis purified water), snap-frozen in dry ice in 2 mL cryogenic tubes, and stored at −80 °C until sample extraction for metabolomics analysis.

2.4. Metabolite extraction

The extraction method was adapted from Raldúa D. et al. (Raldúa et al., 2020). In brief, zebrafish larvae were homogenized in 500 μL of pre-chilled $CHCl_3$:MeOH (2:1, v/v) and 20 μL of IS solution, with two 5 mm stainless beads using a TissueLyser (Qiagen, CA, USA) at 50 Hz for 4 min. Resulting homogenates were transferred to a 2 mL cryogenic tube, mixed with 117 μL of pre-chilled ultrapure water and shaken for 20 min. After centrifugation (14,680 rpm, 4 °C, 20 min), 100 μL of the upper aqueous fraction were transferred into amber chromatographic vials for further LC-MS analysis. For quality control assurance we prepared an extraction blank and a quality control (QC) sample by pooling 10 μL of each extract.

2.5. LC-MS and MS/MS analysis

Untargeted metabolomics analyses were performed by injecting 3 μL of the aqueous extracts in a 1290 UHPLC system coupled to a 6550 quadrupole time of flight (QTOF) mass spectrometer, both from Agilent Technologies (Palo Alto, CA, USA), operated in positive electrospray ionization mode (ESI+). LC-MS conditions were adapted from Torres S. et al. (Torres et al., 2021). Briefly, chromatographic separation was conducted on a Luna® Omega Polar C_{18} column (1.6 μm, 150 × 2.1 mm, 100 Å, Phenomenex, CA, USA) at a flow rate of 0.450 mL min^{-1}. Column temperature was set to 30 °C. The mobile phases were 0.1% formic acid in Milli-Q water (A), and 0.1% formic acid in acetonitrile (B). The linear gradient elution started at 100% of A (time 0–2 min), 100% of A to 100% of B (2–9 min), 100% of B (9–10 min) and finished at 100% of A (10–12 min) followed by 4 min post-run time. ESI conditions were gas temperature, 150 °C; drying gas, 11 L min^{-1}; nebulizer, 30 psig; fragmentor, 120 V; and skimmer, 65 V. Mass spectra were acquired over the *m/z* range 50–1000 at 3 spectra s^{-1}. Prior to sample analysis, we performed four column blanks until signal stabilisation, followed by the analysis of the extraction blank, and the injection of the QC until signal stabilisation (five times). All samples (five replicates per treatment, 25 samples in total) were randomly injected. Instrument performance was monitored by the injection of the QC at the beginning of the sequence and periodically every five samples.

For identification purposes, targeted MS/MS towards protonated ionic species from relevant features were performed under the same chromatographic conditions at fixed collision energies of 10, 20, 30 and 40 V. The instrument was set to acquire the selected precursor ions over the *m/z* range of 40–1000 with a narrow isolation window width of 1.3 *m/z*.

2.6. Data processing and statistical analysis

Differences in developmental anomalies were evaluated using Z-test of proportions. LC-MS raw data was converted into mzXML format via MSconvert software from Proteowizard (Holman et al., 2014) and then processed using the XCMS software (version 3.8.2) to detect and align features (Smith et al., 2006). An intensity threshold above 5000 counts and a relative standard deviation higher than in QC were used as criteria to retain features for downstream statistical analysis. Feature matrix intensities were normalized using Probabilistic Quotient Normalization (PQN) to account for sample dilution (Dieterle et al., 2006; Guida et al., 2016). Samples were further normalized using the number of zebrafish embryos before entering a principal component analysis (PCA) for initial inspection of the different exposure level groups. One-way ANOVA with false discovery rate (FDR) control was used to study differences across exposure levels ($p < 0.05$ were considered for significance in all statistical tests). The heatmap with hierarchical clustering of the identified metabolites was performed using Pheatmap package version 1.0.12 (Kolde, 2019). Figures were created using ggplot2 version 3.3.0 (Wickham, 2011). Data processing and analysis was conducted in R version 3.6.3 (R Core Team, 2021).

2.7. Metabolite identification and pathway analysis

Statistically relevant features were putatively annotated by searching against the HMDB version 4.0 (Wishart et al., 2018), and an in-house compiled list of previously reported NNK metabolites summarised in Table S2 (Dator et al., 2018; Hecht, 1998) considering the exact mass of their protonated adduct within 5 ppm mass error. Confirmation of the annotations was performed by matching their experimental MS/MS spectra and retention time with the MS/MS and retention time of their pure chemical standards (level 1 of confirmation according to Schymanski et al. (Schymanski et al., 2014)). When pure chemical standards were not available, metabolic annotation (Nash and Dunn, 2019) was performed by comparing our experimental MS/MS spectra with experimental MS/MS spectra available in the METLIN (Smith et al., 2005) and MoNA (MoNA: MassBank of North America, 2021) databases, or with MS/MS data from the bibliography (Dator et al., 2018) (level 2 of identification confirmation). Identifications were used to feed a graphical network-based pathway enrichment analysis via FELLA package version 1.10.0 (Picart-Armada et al., 2018) using *Danio rerio* as a background organism. Diffusion analysis method was performed with the top 150 z-score to prioritise affected KEGG pathways upon NNK exposure considering a p-score < 0.05 for significance.

3. Results and discussion

3.1. NNK embryotoxicity

Fig. 1 shows the phenotypic observations of the different zebrafish groups at 72, 96, and 120 hpf. NNK exposure increased embryo death in a concentration- and time-dependent manner. Based on lethality data, 200 μM was identified as the lowest observed adverse effect level (LOAEL) from 72 to 120 hpf, yet increased developmental abnormalities (spinal cord modifications, development of oedema, and unhatched embryos) were observable in embryos exposed to concentrations ranging from 50 to 100 μM NNK after 96 and 120 hpf (Fig. 1). Our observations are in line with previous reports in mice, demonstrating NNK to be a weak inducer of developmental defects in the progeny of CD1 pregnant mice and in an in vitro assay using mice embryos exposed to 10 and 100 μM NNK (Winn et al., 1998).

3.2. NNK metabolism suspect screening

To assess NNK specific metabolism in zebrafish embryos, a suspect screening analysis for the 23 NNK metabolites was performed resulting in the identification of NNK and two NNK metabolites namely 4-Hydroxy-4-(3-pyridyl)-butyric acid (HPBA) and 4-(Methylnitrosamino)-1-(3-pyridyl-N-oxide)-1-butanol (NNAL-*N*-oxide) (Table S2). Both NNK and HPBA were shown to accumulate in zebrafish embryos in a concentration-dependent manner, while NNAL-*N*-oxide reached a plateau at 100 μM (Fig. 2). The accumulation of these three compounds in zebrafish embryos indicates the absorption and metabolization of NNK by our zebrafish model. NNK absorption and metabolization has been previously demonstrated in human cells, tissues from murine foetuses, and in adult murine models (Hecht, 1998; Jalas et al., 2005; Rossignol et al., 1989). However, this is the first evidence demonstrating NNK to be metabolized by a zebrafish model at early developmental stages. Our results showed HPBA to be significantly increased in all NNK exposed groups respective to the control group. In humans (Wang et al., 2019) and rodent models (Schrader et al., 1998), HPBA is a product of NNK metabolic activation leading to NNAL formation followed by CYP450-mediated α-hydroxylation of its carbon adjacent to the nitrosamino group (Smith et al., 1992). Of note, it has been recently demonstrated that various drug-metabolizing CYPs are expressed in zebrafish embryos and larvae and that their metabolic activity resembles those of human CYP isoforms (Nawaji et al., 2020). This CYP450-mediated α-hydroxylation can lead to the formation of reactive

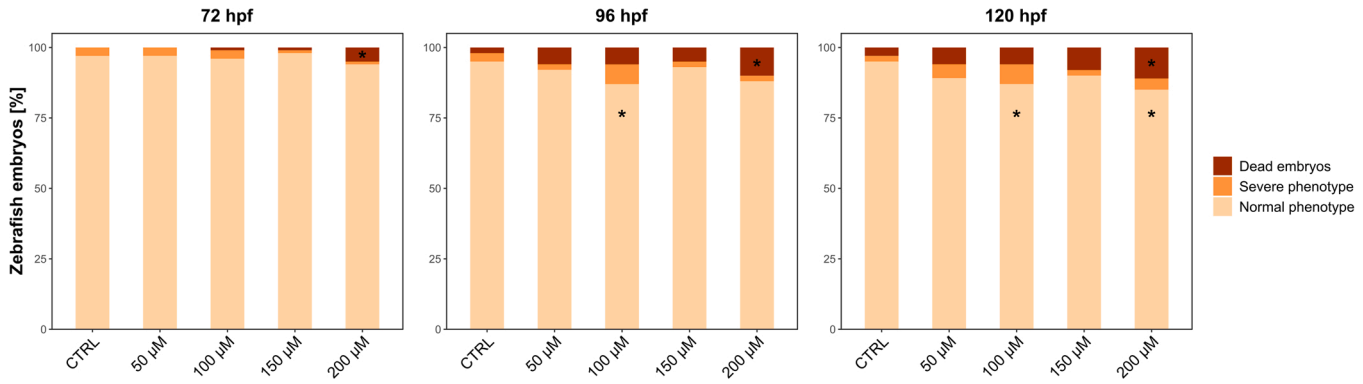

Fig. 1. Phenotypic observations of zebrafish embryos exposure groups at 72, 96 and 120 hpf. Observations were based on normal phenotype, severe phenotype (non-hatched embryos, oedema, and abnormalities in morphology) and dead embryos. Asterisks denote statistical significance according to a Z-test compared against the control group; * p-value < 0.05. CTRL: control, non-exposed group; 50 µM, 100 µM, 150 µM, 200 µM: groups exposed to the respective NNK concentration.

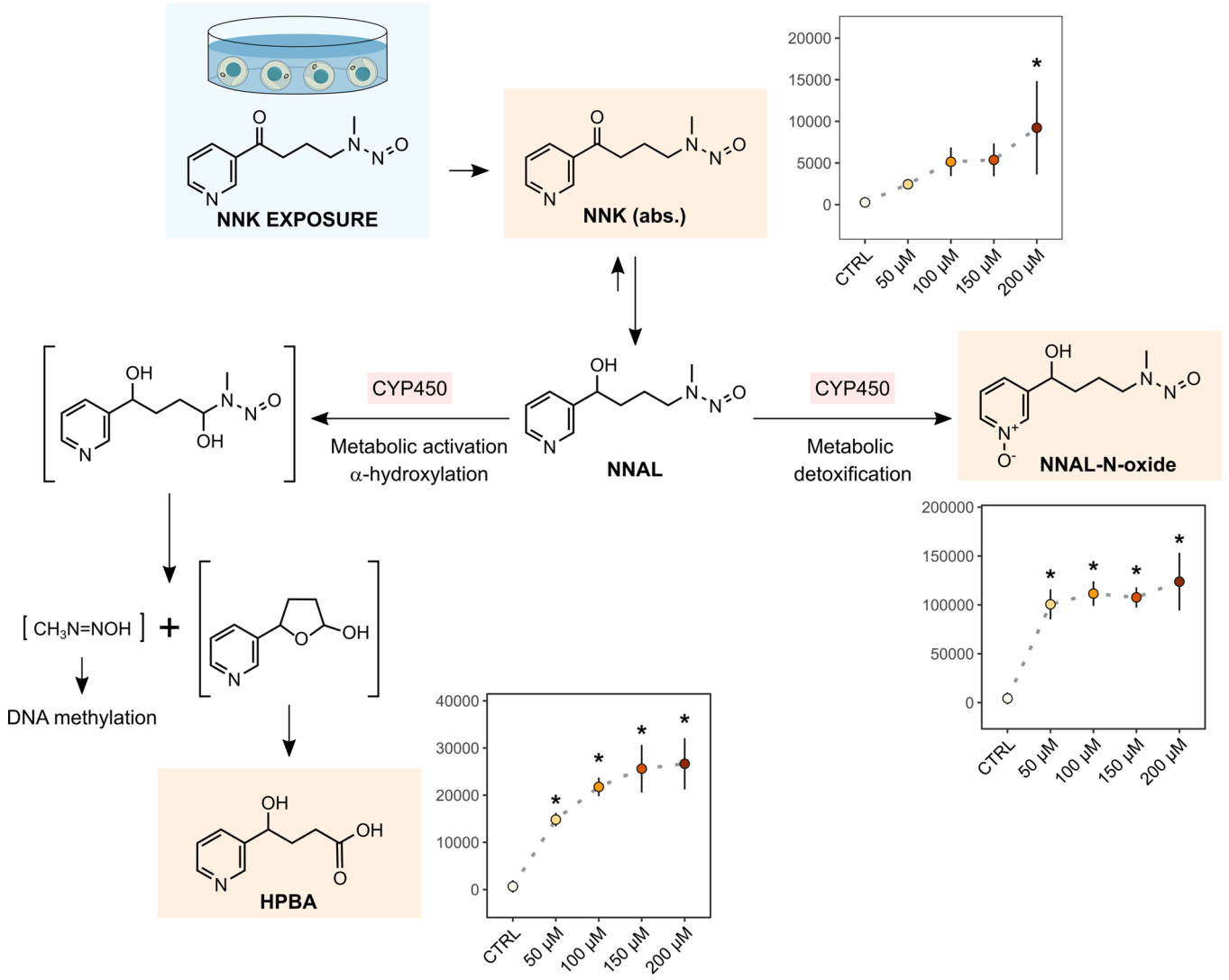

Fig. 2. Trends of NNK derived metabolites identified in the exposed groups and their role in the NNK metabolism. After absorption, NNK is transformed to NNAL followed by a detoxification process through NNAL-*N*-oxide and a metabolic activation through the α-hydroxylation pathway that results in the generation of HPBA. Each point represents the mean intensities per group and the error bar represents the standard deviation (n = 5 samples per group). Detected metabolites are those marked with a beige background. Asterisks denote statistical significance according to a multiple group comparison of ANOVA (only significative results of exposed groups vs control are illustrated); * p-value < 0.05. NNK: 4-(methylnitrosamino)-1-(3-pyridyl)-1-butanone; NNAL-*N*-Oxide: 4-(Methylnitrosamino)-1-(3-pyridyl-N-oxide)-1-butanol; HPBA: 4-Hydroxy-4-(3-pyridyl)-butyric acid. NNK metabolism representation adapted from Hecht S. (Hecht, 1998).(For interpretation of the references to colour in this figure legend, the reader is referred to the web version of this article.)

intermediates that react with DNA forming methyl (i.e., O^6-mdG, 7-mdG), pyridyloxobutyl (POB, O^6-POB-dG) or/and pyridylhydroxybutyl (PHB) DNA adducts which are critical in carcinogenesis (Balbo et al., 2014; Hang, 2010; Hecht et al., 2016; Hecht, 1999) (Fig. 2). Our results also indicate that our zebrafish embryo model is undergoing an NNK detoxification process as suggested by the formation of NNAL-*N*--oxide which is the product of the pyridine-*N*-oxidation reaction of NNAL mediated by P450 enzymes (CYP450) (Carmella et al., 1997; Perez-Paramo et al., 2019).

3.3. NNK-related metabolic disruptions

Metabolic disruptions occurring upon NNK exposure during early development were assayed using an untargeted metabolomics approach and results are summarized in Fig. 3. Fig. 3A displays the PC1 vs PC2 score plot of the PCA performed on the filtered and normalized metabolic features revealing an NNK concentration-dependent clustering trend along PC1 gathering 25% of explained variance. An overlap of those embryo replicates exposed to the two highest NNK concentrations (150 and 200 μM) is also evidenced, indicating similarities in the metabolic response of the embryos exposed at these concentrations. Metabolic features accounting for significant differences in a one-variable-at-a-time one-way ANOVA comparison ($p < 0.05$) were used for MS/MS identification. We confirmed the identity of 21 metabolites (Table 1) including amino acids such as methionine, dipeptides, fatty acid esters, nucleobases such as guanine and uracil, nucleosides such as guanosine, inosine, and uridine, and nucleotides such as CMP, GMP, and UMP. A heatmap representation of intensity levels for these 21 metabolites is displayed in Fig. 3B, showing three clusters of samples corresponding to the non-exposed embryos, those exposed to the lowest (50 and 100 μM), and those exposed to the highest NNK concentrations (150 and 200 μM) in line with the results of the PCA analysis.

The 21 identified metabolites were used as input to the network-based enrichment analysis (Fig. 3C) showing that three main metabolic pathways were influenced by the exposure to NNK in early development (p-score < 0.05): purine and pyridine metabolisms, and base excision repair (BER) pathway. Some metabolites belonging to purine metabolism, such as hypoxanthine, inosine, guanine, and

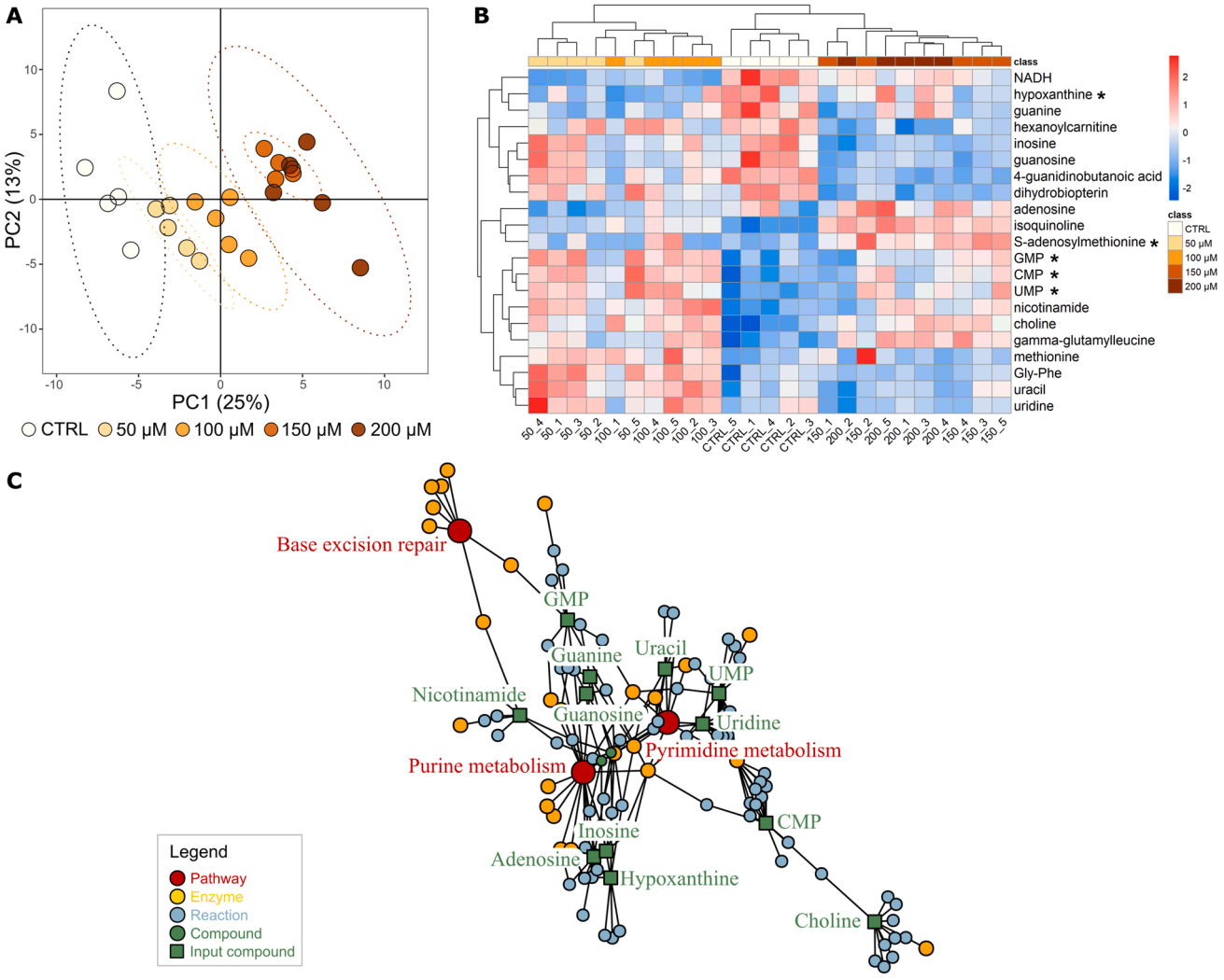

Fig. 3. Metabolomic results of the molecular phenotype. (A) Unsupervised PCA analysis of metabolomics data. PCA score plot was generated from 2751 features detected in control and NNK exposed groups after data filtering and normalization. (B) Heatmap and hierarchical clustering of identified endogenous metabolites. Each column represents the relative intensity of each metabolite per sample after standard scaling. Asterisks denote metabolites with level 1 identification. (C) Network-based pathway enrichment by FELLA of significant endogenous metabolites altered by NNK exposure using the top 150 z-score for diffusion analysis. Red circles represent the enriched pathways, and yellow, blue, and green circles represent the potential enzymes, reactions, and compounds to also be affected. Green squares represent the input metabolites to the enriched pathways.

Table 1
List of the identified endogenous metabolites altered in zebrafish embryos exposed to NNK, their KEEG ID when available, FDR adjusted p-value, and identification level (ID level) accordingly with Schymanski et al. (Schymanski et al., 2014). Those metabolites identifications confirmed with the pure chemical standard are marked in bold.

Metabolite	KEEG ID	FDR p-value	ID level
4-guanidinobutanoic acid	C01035	5.60×10^{-6}	2
adenosine	C00212	4.69×10^{-2}	2
choline	C00114	3.18×10^{-5}	2
cytidine monophosphate (CMP)	C00055	1.87×10^{-3}	1
dihydrobiopterin	C02953	4.18×10^{-4}	2
gamma-glutamylleucine	–	1.31×10^{-3}	2
glycylphenylalanine (Gly-Phe)	–	2.28×10^{-4}	2
guanosine monophosphate (GMP)	C00144	1.88×10^{-2}	1
guanine	C00242	3.21×10^{-3}	2
guanosine	C00387	1.08×10^{-2}	2
hexanoylcarnitine	–	5.53×10^{-3}	2
hypoxanthine	C00262	3.96×10^{-2}	1
inosine	C00294	7.05×10^{-3}	2
isoquinoline	C06323	1.60×10^{-10}	2
methionine	C00073	5.93×10^{-2}	2
Reduced nicotinamide adenine dinucleotide (NADH)	C00004	5.29×10^{-5}	2
nicotinamide	C00153	3.64×10^{-3}	2
S-adenosylmethionine	C00019	1.30×10^{-2}	1
uridine monophosphate (UMP)	C00105	6.98×10^{-3}	1
uracil	C00106	7.94×10^{-3}	2
uridine	C00299	2.39×10^{-2}	2

guanosine, followed a decreasing trend as the concentration of NNK exposure increased (Fig. S1A). In contrast, intensities of pyrimidines such as uracil and uridine showed a sharp increase at the lowest exposure concentration (50 μM) and a progressive decrease with increased NNK concentrations (Fig. S1B). The RNA monomers CMP, GMP and UMP followed this same trend, maintaining significantly increased concentrations respective to controls and peaking at 50 μM (Fig. 4). Different changes in the metabolites related to the purine metabolism were also induced by nicotine exposure in adult zebrafish skeletal muscle (Gómez-Canela et al., 2018). Increased ribonucleotide biosynthesis has been linked to carcinogenic processes, which require elevated rates of RNA synthesis (Bywater et al., 2013; Villicaña et al., 2014). On the other hand, our results suggest a significant alteration of BER pathway activity upon NNK exposure, an effect not observed in mice models (Gupta et al., 2013). BER pathway is one of the primary repair mechanisms for the removal of small DNA lesions such as alkylated, oxidized, and deaminated bases from endogenous sources or environmental carcinogens, i.e., non-bulky adducts such as those produced by NNK (Hang, 2010; Peterson, 2010).

4. Conclusions

Our results demonstrate, for the first time, the impact of NNK exposure to zebrafish embryos. Based on lethality, a LOAEL of 200 μM was observed from 72 to 120 hpf. Besides the detection of NNK, the detection of HPBA and NNAL-*N*-oxide in zebrafish extracts confirmed the ability of our zebrafish embryo model to absorb and metabolize NNK. We suggest the activation of two parallel pathways: NNK detoxification through NNAL-*N*-oxide formation and CYP450-mediated α-hydroxylation forming reactive intermediates that cause DNA-adducts eventually driving carcinogenesis. We demonstrated these to be paralleled by activation of the BER pathway that counteracts genome instability caused by DNA-lesions occurring upon NNK exposure. Additionally, this is also accompanied by a disruption of purine and pyrimidine metabolisms with nucleotide biosynthesis increasing at the lowest NNK exposure concentration. Altogether, results obtained from this exploratory study confirm NNK to be a harmful embryonic agent. Besides, they demonstrate zebrafish embryos to be a suitable early development model to monitor NNK toxicity reproducing effects previously observed in vitro and in higher order vertebrate models. Further studies are warranted towards targeting small DNA-lesions corrected by BER pathway such as oxidation (i.e., 8-Oxoguanine, 5-Hydroxycytosine) or alkylation (i.e., 3-Methylguanine, 3-Methyladenine), and towards the determination of the specific NNK metabolizing CYP450s in zebrafish

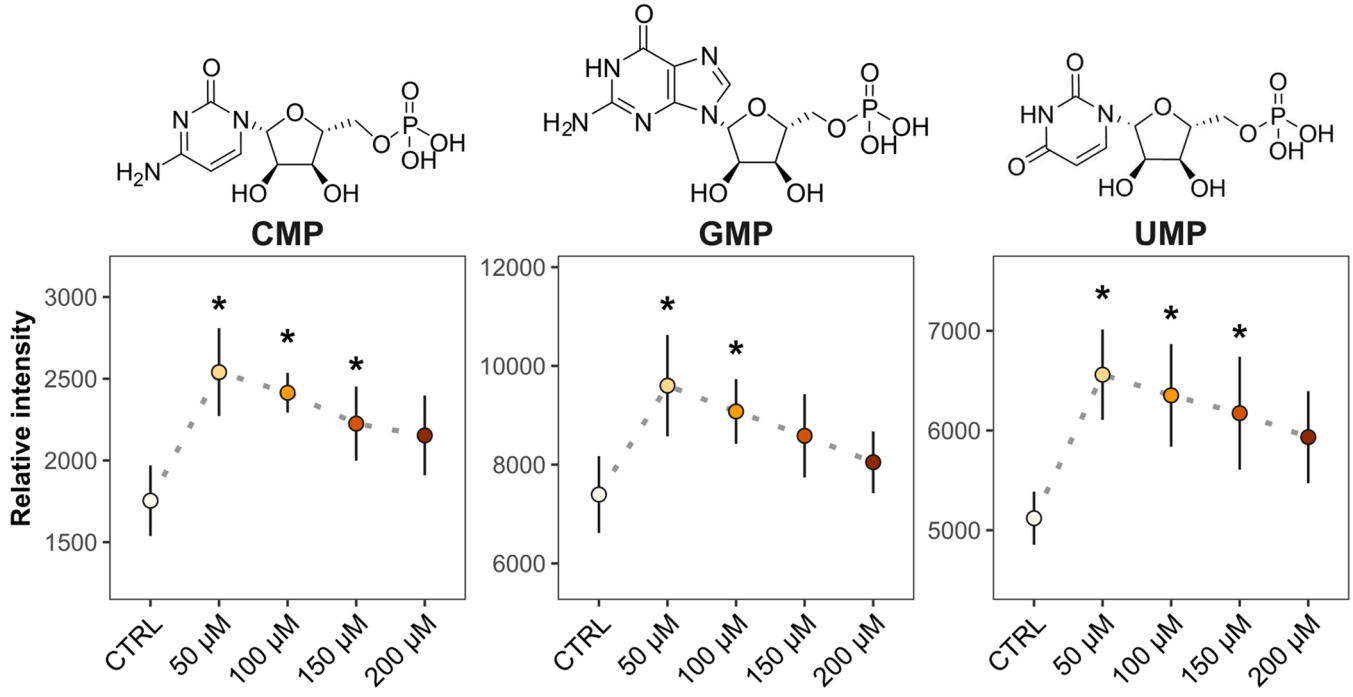

Fig. 4. Identified nucleotide monophosphates significantly altered by NNK exposure. Each point represents the mean intensities and the error bars represent the standard deviation (n = 5 samples). Asterisks denote statistical significance according to a multiple group comparison of ANOVA (only significative results of exposed groups vs control are illustrated); * p-value < 0.05.

embryos.

CRediT authorship contribution statement

Carla Merino: Software, Validation, Formal analysis, Investigation, Data curation, Writing – original draft; Visualization. **Marta Casado:** Methodology, Resources, Investigation. **Benjamí Piña:** Conceptualization, Methodology, Resources, Writing – review & editing. **Maria Vinaixa:** Conceptualization, Formal analysis, Writing - Original draft, Writing – review & editing, Visualization, Supervision. **Noelia Ramírez:** Conceptualization, Investigation, Supervision, Writing – review & editing, Project administration, Funding acquisition.

Declaration of Competing Interest

The authors declare that they have no known competing financial interests or personal relationships that could have appeared to influence the work reported in this paper.

Data availability

Raw mass spectrometry data files (mzXML) and the RMarkdown file containing code to reproduce data analysis are available at Zenodo with ID number 4775188 (DOI: 10.5281/zenodo.4775188)

Acknowledgements

This research was funded by the Secretaria d'Universitats i Recerca del Departament d'Empresa i Coneixement de la Generalitat de Catalunya through C.M.'s predoctoral grant number 2020 FI_B2 00118 and the Spanish Ministry of Science & Innovation through RTI2018–096175-B-I00 (B.P., M.C.), N.R.'s Juan de la Cierva Incorporación grant No. (IJCI-2015–23158), and N.R.'s Miguel Servet contract (CP19/00060) from Instituto de Salud Carlos III, co-financed by Fondo Europeo de Desarrollo Regional (FEDER), Unión Europea, "Una manera de hacer Europa".

Appendix A. Supporting information

Supplementary data associated with this article can be found in the online version at doi:10.1016/j.jhazmat.2021.127746.

References

Anderson, L.M., Hecht, S.S., Dixon, D.E., Dove, L.F., Kovatch, R.M., Amin, S., Hoffmann, D., Rice, J.M., 1989. Evaluation of the transplacental tumorigenicity of the tobacco-specific carcinogen 4-(methylnitrosamino)-l-(3-pyridyl)-l-butanone in mice. Cancer Res. 49, 3770–3775.

Anderson, L.M., Hecht, S.S., Kovatch, R.M., Amin, S., Hoffmann, D., Rice, J.M., 1991. Tumorigenicity of the tobacco-specific carcinogen 4-(methyl-nitrosamino)-1-(3-pyridyl)-1-butanone in infant mice. Cancer Lett. 58, 177–181. https://doi.org/10.1016/0304-3835(91)90097-2.

Balbo, S., James-Yi, S., Johnson, C.S., O'Sullivan, M.G., Stepanov, I., Wang, M., Bandyopadhyay, D., Kassie, F., Carmella, S., Upadhyaya, P., Hecht, S.S., 2013. (S)-N′-nitrosonornicotine, a constituent of smokeless tobacco, is a powerful oral cavity carcinogen in rats. Carcinogenesis 34, 2178–2183. https://doi.org/10.1093/carcin/bgt162.

Balbo, S., Johnson, C.S., Kovi, R.C., James-Yi, S.A., Gerard O'Sullivan, M., Wang, M., Le, C.T., Khariwala, S.S., Upadhyaya, P., Hecht, S.S., 2014. Carcinogenicity and DNA adduct formation of 4-(methylnitrosamino)-1-(3-pyridyl)- 1-butanone and enantiomers of its metabolite 4-(methylnitrosamino)-1-(3-pyridyl)-1- butanol in F-344 rats. Carcinogenesis 35, 2798–2806. https://doi.org/10.1093/carcin/bgu204.

Bywater, M.J., Pearson, R.B., McArthur, G.A., Hannan, R.D., 2013. Dysregulation of the basal RNA polymerase transcription apparatus in cancer. Nat. Rev. Cancer. https://doi.org/10.1038/nrc3496.

Carmella, S.G., Borukhova, A., Akerkar, S.A., Hecht, S.S., 1997. Analysis of human urine for pyridine-N-oxide metabolites of 4-(methylnitrosamino)-1-(3-pyridyl)-1-butanone, a tobacco-specific lung carcinogen. Cancer Epidemiol. Biomark. Prev. 6, 113–120.

Cheng, G., Li, J., Zheng, M., Zhao, Y., Zhou, J., Li, W., 2015. NNK, a tobacco-specific carcinogen, inhibits the expression of lysyl oxidase, a tumor suppressor. Int. J. Environ. Res. Public Health 12, 64–82. https://doi.org/10.3390/ijerph120100064.

Correa, E., Joshi, P.A., Castonguay, A., Schüller, H.M., 1990. The tobacco-specific nitrosamine 4-(Methylnitrosamino)-l-(3-pyridyl)-l-butanone is an active transplacental carcinogen in Syrian golden hamsters. Cancer Res 50, 3435–3438.

Dator, R., Von Weymarn, L.B., Villalta, P.W., Hooyman, C.J., Maertens, L.A., Upadhyaya, P., Murphy, S.E., Balbo, S., 2018. In vivo stable-isotope labeling and mass-spectrometry-based metabolic profiling of a potent tobacco-specific carcinogen in rats. Anal. Chem. 90, 11863–11872. https://doi.org/10.1021/acs.analchem.8b01881.

Dieterle, F., Ross, A., Schlotterbeck, G., Senn, H., 2006. Probabilistic quotient normalization as robust method to account for dilution of complex biological mixtures. Application in 1H NMR metabonomics. Anal. Chem. 78, 4281–4290. https://doi.org/10.1021/AC051632C.

Farren, N.J., Ramírez, N., Lee, J.D., Finessi, E., Lewis, A.C., Hamilton, J.F., 2015. Estimated exposure risks from carcinogenic nitrosamines in urban airborne particulate matter. Environ. Sci. Technol. 49, 9648–9656. https://doi.org/10.1021/acs.est.5b01620.

Gómez-Canela, C., Prats, E., Lacorte, S., Raldúa, D., Piña, B., Tauler, R., 2018. Metabolomic changes induced by nicotine in adult zebrafish skeletal muscle. Ecotoxicol. Environ. Saf. 164, 388–397. https://doi.org/10.1016/j.ecoenv.2018.08.042.

Guida, R.Di, Engel, J., Allwood, J.W., Weber, R.J.M., Jones, M.R., Sommer, U., Viant, M. R., Dunn, W.B., 2016. Non-targeted UHPLC-MS metabolomic data processing methods: a comparative investigation of normalisation, missing value imputation, transformation and scaling. Metabolomics 12. https://doi.org/10.1007/S11306-016-1030-9.

Gupta, N., Curtis, R.M., Mulder, J.E., Massey, T.E., 2013. Acute in vivo treatment with 4-(methylnitrosamino)-1-(3-pyridyl)-1-butanone does not alter base excision repair activities in murine lung and liver. DNA Repair 12, 1031–1036. https://doi.org/10.1016/j.dnarep.2013.09.009.

Hang, B., 2010. Formation and repair of tobacco carcinogen-derived bulky DNA adducts. J. Nucleic Acids. https://doi.org/10.4061/2010/709521.

Hang, B., Sarker, A.H., Havel, C., Saha, S., Hazra, T.K., Schick, S., Jacob, P., Rehan, V.K., Chenna, A., Sharan, D., Sleiman, M., Destaillats, H., Gundel, L.A., 2013. Thirdhand smoke causes DNA damage in human cells. Mutagenesis 28, 381–391. https://doi.org/10.1093/mutage/get013.

Hartung, T., 2009. Toxicology for the twenty-first century. Nature 460, 208–212. https://doi.org/10.1038/460208a.

Hecht, S.S., 1998. Biochemistry, biology, and carcinogenicity of tobacco-specific N-nitrosamines. Chem. Res. Toxicol. 11, 559–603. https://doi.org/10.1021/tx980005y.

Hecht, S.S., 1999. DNA adduct formation from tobacco-specific N-nitrosamines. Mutat. Res. 424, 127–142. https://doi.org/10.1016/S0027-5107(99)00014-7.

Hecht, S.S., Hoffmann, D., 1988. Tobacco-specific nitrosamines, an important group of carcinogens in tobacco and tobacco smoke. Carcinogenesis 9 (6), 875–884. https://doi.org/10.1093/carcin/9.6.875.

Hecht, S.S., Stepanov, I., Carmella, S.G., 2016. Exposure and metabolic activation biomarkers of carcinogenic tobacco-specific nitrosamines. Acc. Chem. Res. 49, 106–114. https://doi.org/10.1021/acs.accounts.5b00472.

Holman, J.D., Tabb, D.L., Mallick, P., 2014. Employing ProteoWizard to convert raw mass spectrometry data. Curr. Protoc. Bioinforma. 46 https://doi.org/10.1002/0471250953.bi1324s46.

International Agency for Reasearch on Cancer, 2007. IARC Monographs on the Evaluation of Carcinogenic Risks to Humans Smokeless Tobacco and Some. In: Tobacco-specific N-Nitrosamines, 89. Lyon, France.

Jacob, P., Benowitz, N.L., Destaillats, H., Gundel, L., Hang, B., Martins-Green, M., Matt, G.E., Quintana, P.J.E., Samet, J.M., Schick, S.F., Talbot, P., Aquilina, N.J., Hovell, M.F., Mao, J.H., Whitehead, T.P., 2017. Thirdhand smoke: new evidence, challenges, and future directions. Chem. Res. Toxicol. 30, 270–294. https://doi.org/10.1021/acs.chemrestox.6b00343.

Jalas, J.R., Hecht, S.S., Murphy, S.E., 2005. Cytochrome P450 enzymes as catalysts of metabolism of 4-(methylnitrosamino) -1-(3-pyridyl)-1-butanone, a tobacco specific carcinogen. Chem. Res. Toxicol. https://doi.org/10.1021/tx049847p.

Jarque, S., Rubio-Brotons, M., Ibarra, J., Ordoñez, V., Dyballa, S., Miñana, R., Terriente, J., 2020. Morphometric analysis of developing zebrafish embryos allows predicting teratogenicity modes of action in higher vertebrates. Reprod. Toxicol. 96, 337–348. https://doi.org/10.1016/j.reprotox.2020.08.004.

Lai, F.Y., Lympousi, K., Been, F., Benaglia, L., Udrisard, R., Delémont, O., Esseiva, P., Thomaidis, N.S., Covaci, A., van Nuijs, A.L.N., 2018. Levels of 4-(methylnitrosamino)-1-(3-pyridyl)-1-butanone (NNK) in raw wastewater as an innovative perspective for investigating population-wide exposure to third-hand smoke. Sci. Rep. 8, 1–9. https://doi.org/10.1038/s41598-018-31324-6.

Lieschke, G.J., Currie, P.D., 2007. Animal models of human disease: Zebrafish swim into view. Nat. Rev. Genet 8, 353–367. https://doi.org/10.1038/nrg2091.

Matt, G.E., Quintana, P.J.E., Destaillats, H., Gundel, L. a, Sleiman, M., Singer, B.C., Jacob, P., Benowitz, N., Winickoff, J.P., Rehan, V., Talbot, P., Schick, S., Samet, J., Wang, Y., Hang, B., Martins-Green, M., Pankow, J.F., Hovell, M.F., 2011. Thirdhand tobacco smoke: Emerging evidence and arguments for a multidisciplinary research agenda. Environ. Health Perspect. 119, 1218–1226. https://doi.org/10.1289/ehp.1103500.

Kolde, R., 2019. Pheatmap: Pretty heatmaps R Package. Version 1.0.12. https://rdrr.io/cran/pheatmap/ (Acessed October 2021).

MoNA: MassBank of North America, 2021. Available from: ⟨https://mona.fiehnlab.ucdavis.edu/⟩ (accessed 17 February 2021).

Nash, W.J., Dunn, W.B., 2019. From mass to metabolite in human untargeted metabolomics: Recent advances in annotation of metabolites applying liquid

chromatography-mass spectrometry data. Trends Anal. Chem. 120, 115324 https://doi.org/10.1016/j.trac.2018.11.022.
National Research Council, 2007. Toxicity testing in the 21st century: a vision and a strategy. National Academies Press. https://doi.org/10.17226/11970.
Nawaji, T., Yamashita, N., Umeda, H., Zhang, S., Mizoguchi, N., Seki, M., Kitazawa, T., Teraoka, H., 2020. Cytochrome P450 expression and chemical metabolic activity before full liver development in Zebrafish. Pharmaceuticals 13, 1–17. https://doi.org/10.3390/ph13120456.
Perez-Paramo, Y.X., Watson, C.J.W., Xia, Z., Chen, G., Lazarus, P., 2019. Cytochrome P450 enzyme contributions to the N-oxide detoxification pathway of tobacco-specific nitrosamines; a possible role in tobacco-related cancer risk. FASEB J. 33 https://doi.org/10.1096/FASEBJ.2019.33.1_SUPPLEMENT.508.8.
Peterson, L.A., 2010. Formation, repair, and genotoxic properties of bulky DNA adducts formed from tobacco-specific nitrosamines. J. Nucleic Acids. https://doi.org/10.4061/2010/284935.
Picart-Armada, S., Fernández-Albert, F., Vinaixa, M., Yanes, O., Perera-Lluna, A., 2018. FELLA: an R package to enrich metabolomics data. BMC Bioinforma. 19, 538. https://doi.org/10.1186/s12859-018-2487-5.
R Core Team, 2021. R: A language and environment for statistical computing. R Foundation for Statistical Computing, Vienna, Austria. https://www.R-project.org/.
Raldúa, D., Casado, M., Prats, E., Faria, M., Puig-Castellví, F., Pérez, Y., Alfonso, I., Hsu, C.Y., Arick, M.A., Garcia-Reyero, N., Ziv, T., Ben-Lulu, S., Admon, A., Piña, B., 2020. Targeting redox metabolism: the perfect storm induced by acrylamide poisoning in the brain. Sci. Rep. 10, 312. https://doi.org/10.1038/s41598-019-57142-y.
Ramirez, T., Daneshian, M., Kamp, H., Bois, F.Y., Clench, M.R., Coen, M., Donley, B., Fischer, S.M., Ekman, D.R., Fabian, E., Guillou, C., Heuer, J., Hogberg, H.T., Jungnickel, H., Keun, H.C., Krennrich, G., Krupp, E., Luch, A., Noor, F., Peter, E., Riefke, B., Seymour, M., Skinner, N., Smirnova, L., Verheij, E., Wagner, S., Hartung, T., Van Ravenzwaay, B., Leist, M., 2013. Metabolomics in toxicology and preclinical research. ALTEX 30, 209–225. https://doi.org/10.14573/altex.2013.2.209.
Ramírez, N., Özel, M.Z., Lewis, A.C., Marcé, R.M., Borrull, F., Hamilton, J.F., 2014. Exposure to nitrosamines in thirdhand tobacco smoke increases cancer risk in non-smokers. Environ. Int. 71, 139–147. https://doi.org/10.1016/j.envint.2014.06.012.
Rossignol, G., Alaoui-Jamali, M.A., Castonguay, A., Schuller, H.M., 1989. Metabolism and DNA Damage Induced by 4-(Methylnitrosamino)-l-(3-pyridyl)-l-butanone in Fetal Tissues of the Syrian Golden Hamster. CANCER Res 49, 5671–5676.
Schick, S.F., Glantz, S., 2007. Concentrations of the carcinogen 4-(methylnitrosamino)-1-(3-pyridyl)-1-butanone in sidestream cigarette smoke increase after release into indoor air: Results from unpublished tobacco industry research. Cancer Epidemiol. Biomark. Prev. 16, 1547–1553. https://doi.org/10.1158/1055-9965.EPI-07-0210.
Schrader, E., Hirsch-Ernst, K.I., Richter, E., Foth, H., 1998. Metabolism of 4-(methylnitrosamino)-1-(3-pyridyl)-1-butanone (NNK) in isolated rat lung and liver. Naunyn Schmiede. Arch. Pharmacol. 357, 336–343.
Schymanski, E.L., Jeon, J., Gulde, R., Fenner, K., Ruff, M., Singer, H.P., Hollender, J., 2014. Identifying small molecules via high resolution mass spectrometry: communicating confidence. Environ. Sci. Technol. https://doi.org/10.1021/es5002105.
Sipes, N.S., Padilla, S., Knudsen, T.B., 2011. Zebrafish-As an integrative model for twenty-first century toxicity testing. Birth Defects Res. Part C Embryo Today Rev. 93, 256–267. https://doi.org/10.1002/bdrc.20214.
Sleiman, M., Gundel, L.A., Pankow, J.F., Jacob, P., Singer, B.C., Destaillats, H., 2010. Formation of carcinogens indoors by surface-mediated reactions of nicotine with nitrous acid, leading to potential thirdhand smoke hazards. Proc. Natl. Acad. Sci. 107, 6576–6581. https://doi.org/10.1073/pnas.0912820107.
Smith, C.A., O'Maille, G., Want, E.J., Qin, C., Trauger, S.A., Brandon, T.R., Custodio, D. E., Abagyan, R., Siuzdak, G., 2005. METLIN: a metabolite mass spectral database. Ther. Drug Monit. 27, 747–751. https://doi.org/10.1097/01.ftd.0000179845.53213.39.
Smith, C.A., Want, E.J., O'Maille, G., Abagyan, R., Siuzdak, G., 2006. XCMS: processing mass spectrometry data for metabolite profiling using nonlinear peak alignment, matching and identification. Anal. Chem. https://doi.org/10.1021/AC051437Y.
Smith, T.J., Guo, Z., Gonzalez, F.J., Guengerich, F.P., Stoner, G.D., Yang, C.S., 1992. Metabolism of 4-(Methylnitrosamino)-1-(3-pyridyl)-1-butanone in human lung and liver microsomes and cytochromes P-450 expressed in hepatoma cells. Cancer Res. 52, 1757–1763.
Torres, S., Samino, S., Ràfols, P., Martins-Green, M., Correig, X., Ramírez, N., 2021. Unravelling the metabolic alterations of liver damage induced by thirdhand smoke. Environ. Int. 146, 106242 https://doi.org/10.1016/j.envint.2020.106242.
U.S. Department of Health and Human Services, Centers for Disease Control and Prevention, National Center for Chronic Disease Prevention, and Health Promotion, Office on Smoking and Health , 2014. The Health Consequences of Smoking - 50 Years of Progress: a Report of the Surgeon General. Atlanta, GA, US.
Villicaña, C., Cruz, G., Zurita, M., 2014. The basal transcription machinery as a target for cancer therapy. Cancer Cell Int. https://doi.org/10.1186/1475-2867-14-18.
Wang, H., Li, X., Zhao, G., Xu, L., Wang, S., Nie, M., Hua, C., Shang, P., Pan, L., Zhao, J., Qiao, L., Liu, K., Hu, K., Su, J., Cai, J., Xie, F., 2019. Analysis of methyl DNA adducts and metabolites in BEAS-2B cells induced by 4-(methylnitrosamino)-1-(3-pyridyl)-1-butanone. Toxicol. Mech. Methods 29, 499–510. https://doi.org/10.1080/15376516.2019.1611982.
Wei, B., Blount, B.C., Xia, B., Wang, L., 2016. Assessing exposure to tobacco-specific carcinogen NNK using its urinary metabolite NNAL measured in US population: 2011-2012. J. Expo. Sci. Environ. Epidemiol. 26, 249–256. https://doi.org/10.1038/jes.2014.88.
Weng, M. wen, Lee, H.W., Park, S.H., Hu, Y., Wang, H.T., Chen, L.C., Rom, W.N., Huang, W.C., Lepor, H., Wu, X.R., Yang, C.S., Tang, shong, M., 2018. Aldehydes are the predominant forces inducing DNA damage and inhibiting DNA repair in tobacco smoke carcinogenesis. Proc. Natl. Acad. Sci. USA 115, E6152–E6161. https://doi.org/10.1073/pnas.1804869115.
Wickham, H., 2011. ggplot2. Wiley Interdisciplinary Reviews: Computational Statistics, pp. 180–185. https://doi.org/10.1002/wics.147.
Winn, L.M., Kim, P.M., Wells, P.G., 1998. Investigation of the tobacco-specific carcinogen 4-(methylnitrosamino)-1-(3-pyridyl)-1-butanone for in vivo and in vitro murine embryopathy and embryonic ras mutations. J. Pharmacol. Exp. Ther. 287, 1128–1135.
Wishart, D.S., Feunang, Y.D., Marcu, A., Guo, A.C., Liang, K., Vázquez-Fresno, R., Sajed, T., Johnson, D., Li, C., Karu, N., Sayeeda, Z., Lo, E., Assempour, N., Berjanskii, M., Singhal, S., Arndt, D., Liang, Y., Badran, H., Grant, J., Serra-Cayuela, A., Liu, Y., Mandal, R., Neveu, V., Pon, A., Knox, C., Wilson, M., Manach, C., Scalbert, A., 2018. HMDB 4.0: the human metabolome database for 2018. Nucleic Acids Res 46, D608–D617. https://doi.org/10.1093/nar/gkx1089.
World Health Organization, 2017. Tobacco and its environmental impact: an overview. World Health Organization.
World Health Organization, 2020. Tobacco. Available from: ⟨https://www.who.int/news-room/fact-sheets/detail/tobacco⟩ (Accessed 29 October 2021).
Wu, J.P., Li, M.H., Chen, J.S., Lee, H.L., 2012. In vivo and in vitro metabolism of tobacco-specific nitrosamine, 4-(methylnitrosamino)-1-(3-pyridyl)-1-butanone (NNK), by the freshwater planarian, Dugesia japonica. Chemosphere 87, 1341–1347. https://doi.org/10.1016/j.chemosphere.2012.02.024.